

Convex Restriction of Power Flow Feasibility Sets

Dongchan Lee , Hung D. Nguyen, Krishnamurthy Dvijotham, and Konstantin Turitsyn

Abstract—The convex restriction of power flow feasibility sets identifies the convex subset of power injections where a solution for power flow equations is guaranteed to exist and satisfy the operational constraints. In contrast to convex relaxations, the convex restriction provides a sufficient condition for power flow feasibility under variations in power generation and demand. In this article, we present a general framework to construct convex restrictions of an algebraic set defined by equality and inequality constraints and apply this framework to the power flow feasibility problem. The procedure results in convex quadratic constraints that provide a sufficiently large region for practical operation of the grid.

Index Terms—AC power flow equations, convex restriction, power grid.

I. INTRODUCTION

OWER-FLOW equations are at the core of steady-state analysis of the power grid [1], [2]. State estimation, security assessment, and optimal power flow (OPF) rely on the ac power flow equations to model the grid. The power flow equations determine internal states of the system, such as voltage magnitudes and phase angles given the profile of generation and loads. While the ac power flow equation provides a standard model for the analysis of the grid, the nonlinearity of the equation creates computational bottlenecks and challenges.

In state estimations and security assessments, the state variables are determined using numerical algorithms, such as the Newton–Raphson method or the backward–forward sweep method. The disadvantage of using a numerical algorithm is that it requires a deterministic operating point to find the exact

Manuscript received February 15, 2019; accepted July 6, 2019. Date of publication July 24, 2019; date of current version September 17, 2019. This work was supported in part by the U.S. Department of Energy Office of Electricity as part of the DOE Grid Modernization Initiative and in part by the National Science Foundation Energy, Power, Control and Networks under Award 1809314. Recommended by Associate Editor P. Van Hentenryck. (Corresponding author: Dongchan Lee.)

- D. Lee is with the Department of Mechanical Engineering, Massachusetts Institute of Technology, Cambridge, MA 02139 USA (e-mail: dclee@mit.edu).
- H. D. Nguyen is with the School of Electrical and Electronic Engineering, Nanyang Technological University, Singapore 639798 (e-mail: hunghtd@ntu.edu.sg).
- K. Dvijotham is with the Google Deepmind, N1C 4AG London, U.K. (e-mail: dvij@cs.washington.edu).
- K. Turitsyn was with the Department of Mechanical Engineering, Massachusetts Institute of Technology, Cambridge, MA 02139 USA. He is now with the D. E. Shaw Group, New York, NY 10036 USA (e-mail: turitsyn@gmail.com).

Digital Object Identifier 10.1109/TCNS.2019.2930896

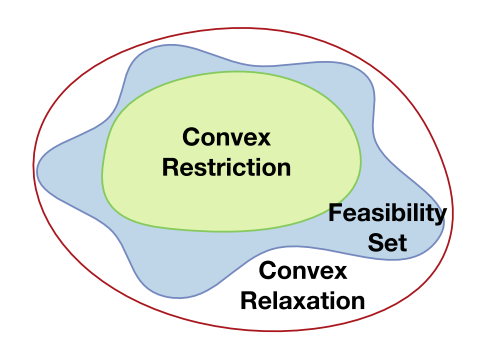


Fig. 1. Illustration of the convex restriction and convex relaxation of a nonconvex feasibility set.

state solution. When uncertainties in the generation and the load profile are introduced, there is no easy way to tell whether there will be a state solution satisfying the ac power flow equations without running an iterative algorithm.

In OPF problems, power flow equations enter as nonlinear equality constraints and result in a nonconvex optimization problem, which is NP-hard [3] even for radial networks [4], [5]. Convex relaxations of power flow equations have been studied extensively for solving OPF problems [5]–[7]. The convex relaxation provides an outer-approximation of the feasibility set, and it is a necessary condition to satisfy the power flow equations. Solving the optimization problem over the relaxed set provides a lower bound on the optimal generation cost, but the resulting solution may not be feasible and risks system security [8]. Moreover, it provides only limited insights and characterizations of the feasibility set because the nonconvex boundaries inside the feasibility set disappear in convex relaxations [9].

This article is concerned with finding the inner approximation of the feasibility set. The *convex restriction* is a convex subset of the feasibility set, which provides a sufficient condition for satisfying power flow equations with operational constraints. Fig. 1 shows the comparison between the convex relaxation and restriction. The benefit of studying the inner approximation is that the security of the system is guaranteed, which is the top priority in the operation of power grids. Moreover, it provides a region where the system is safe to operate, and this region can be used as a metric for robustness against uncertain power injections from renewables and loads. While there are many potential applications of convex restriction, deriving a tractable sufficient condition for the feasibility of the power flow equations has remained a challenge.

2325-5870 © 2019 IEEE. Personal use is permitted, but republication/redistribution requires IEEE permission. See http://www.ieee.org/publications_standards/publications/rights/index.html for more information.

The search for a tractable convex restriction of the power flow equations started in [10] to find the security region where the system is safe to operate. In recent years, a number of efforts have been made to find the inner approximation of the feasibility set, but there has been severe limitations in terms of its applicability to practical systems. Most of the progress was made with certain modeling assumptions, such as a radial topology [11]–[15], a lossless network [16], and a decoupled power flow model [17]. Recent efforts made significant progress with general meshed networks, but they still suffer from poor scalability and conservatism [18]–[20]. In [21], the inner approximation with Brouwer's fixed point theorem showed promising results for general power grid models. However, one of the limitations of this approach was that it required solving a nonconvex optimization problem to construct the convex restriction. In this article, we alleviate this limitation by describing the set in a lifted space and giving a closed-form expression.

We propose an analytical procedure to construct convex restrictions of ac power flow equations with operational constraints. Our technique relies on envelopes over the nonlinearity involved in the power flow equations and the sparse system representation. Our envelopes show an interesting relation to the quadratic convex (QC) relaxation for the OPF problem, which employs convex envelopes to contain the nonlinearities [7], [22]. It will be shown later in this article that the envelopes for restriction have dual features compared to the ones used in relaxations. Moreover, the construction relies on bounds over intervals, which has been studied in interval analysis and uncertainty propagation techniques [23], [24]. The interval analysis also deals with finding the inner approximation of sets described by the constraints, but the study has been limited to a subclass of problems such as linear equations or decentralized nonlinear equations [25]–[27]. To the best of the authors' knowledge, there is no tractable method available that computes the inner approximation of a set defined by general nonlinear equality constraints [24], [26].

Our technique is applied to power systems with a general meshed network without any modification in the system data, and the results are compared with the true feasibility sets obtained by MATPOWER [28]. Our approach achieves drastic improvements on conservatism while retaining scalability to large systems. The main advantages over the existing approaches are summarized as follows.

- The convex restriction is a convex closed-form condition based on the local operating point and does not involve any numerical algorithm. These properties bring advantages to real-time security analysis where computational capability is limited.
- 2) Our method is scalable to large-scale systems. We later show that the number of quadratic constraints grows proportionally to the system size. The convex restriction can be used to solve the OPF problem, replacing the nonconvex power flow equations.
- 3) The convex restriction is guaranteed to be nonempty, given that the system operates in a normal condition. Moreover, the region is nonconservative and provides practical margins for operation. The visualization of this

region shows that the restriction is tight along some of the boundaries in IEEE test cases.

The rest of this article is organized as follows. In Section II, the general formulation of the problem as well as its set-up in power flow equations is provided. Section III provides a guideline for constructing convex restrictions for general constraints. Section IV applies the proposed method to power flow equations and visualizes the comparison between convex restrictions and true feasibility sets. Section V provides the conclusion.

II. CONVEX RESTRICTION OF FEASIBILITY SETS: FORMULATION AND PRELIMINARIES

A. General Formulation

Consider the following general nonlinear equality and inequality constraints with control variables $u \in \mathbf{R}^m$ and state variables $x \in \mathbf{R}^n$

$$f(x,u) = 0 (1a)$$

$$h(x, u) \le 0 \tag{1b}$$

where $f:(\mathbf{R}^n,\mathbf{R}^m)\to\mathbf{R}^n$ and $h:(\mathbf{R}^n,\mathbf{R}^m)\to\mathbf{R}^s$ are vectors of functions that are continuous and differentiable. The variables are divided into control variables and internal states. Control variables are the subset of variables that can be determined freely by the system operators. State variables are the subset of decision variables that are determined by the control variables and the equality constraints in (1a). Notice that the number of equality constraints and the number of state variables are the same. Given the constraints and variables, the solvability and feasibility of control variable u are defined as follows.

Definition 1: u is *solvable* if there exists at least one x that satisfies the equality constraint f(x, u) = 0.

Definition 2: u is *feasible* if there exists at least one x that satisfies f(x,u)=0 and $h(x,u)\leq 0$.

Feasibility and solvability sets refer to the set of all feasible and solvable control variables u. Nonlinear equality constraints create a nonlinear manifold in the space of (x,u), and a singleton (i.e., a set with one element) is the only possible convex inner approximation in a general nonlinear manifold. Instead of working with both x and u, the feasibility set is defined as a projection of the nonlinear manifold onto the control variable space. This set is generally nonconvex, and the goal of this article is to find the convex restriction inside the projection of the nonlinear manifold. The construction of the convex restriction relies on the following assumptions.

Assumption 1: There is a known point (x_0, u_0) that satisfies the following:

- 1) $f(x_0, u_0) = 0, h(x_0, u_0) \le 0$;
- 2) $J_{f,0} = \nabla_x f(x, u_0)|_{x=x_0}$ is nonsingular.

The known operating point (x_0, u_0) will be referred to as the base point.

Remark 1: From the implicit function theorem, there exists an open neighborhood of the solvability set around u_0 when Assumption 1 is satisfied [29].

Moreover, the equation is assumed to have the following sparse representation.

Assumption 2: Nonlinear equations have a sparse nonlinear representation. Namely, there exists a basis function $\psi: (\mathbf{R}^n, \mathbf{R}^m) \to \mathbf{R}^q$ such that

$$f(x,u) = M\psi(x,u)$$

$$h(x,u) = L\psi(x,u)$$
(2)

where $M \in \mathbf{R}^{n \times q}$ and $L \in \mathbf{R}^{r \times q}$ are constant matrices. Moreover, each ψ_k is a function of a finite number of variables independent of n and s.

Many systems of the equations have such sparse representations where the nonlinearity is associated with a small subset of the variables. As an example, we will see that the nonlinearity involved in power flow equations are associated with the transmission lines and the variables involved in the two end nodes of the line. Assumption 2 will later ensure the scalability of the convex restriction.

B. Power Flow Equations and Operational Constraints

Consider a power network as a directed graph $\mathcal{G}(\mathcal{N}, \mathcal{E})$ where each node in \mathcal{N} represents a bus, and each edge in $\mathcal{E} \subseteq \mathcal{N} \times \mathcal{N}$ represents a transmission line. For each transmission line l, we will denote its from bus with superscript f, and its to bus as superscript t. The buses are divided into slack, PV, and PQ buses according to the conventional definitions in power systems. The slack bus is denoted by $\mathcal{N}_{\text{slack}}$ with the given values of voltage magnitude and the reference phase angle. The reference phase angle is assigned to zero. The set of non-slack buses is denoted by $\mathcal{N}_{ns} = \mathcal{N} \setminus \mathcal{N}_{slack}$. The set of PV bues is denoted by \mathcal{N}_{pv} with the given values of the active power injection and the voltage magnitude. The set of PQ bues is denoted by \mathcal{N}_{pq} with the given values of the active and reactive power injections. The set of generator buses is denoted by $\mathcal{N}_G = \mathcal{N}_{pv} \cup \mathcal{N}_{slack}$. Consider the following ac power flow equations in polar coordinates with operational constraints:

$$p_i^{\text{inj}} = \sum_{k \in \mathcal{N}} v_i v_k (G_{ik} \cos \theta_{ik} + B_{ik} \sin \theta_{ik}) \quad i \in \mathcal{N}$$

$$q_i^{\text{inj}} = \sum_{k \in \mathcal{N}} v_i v_k (G_{ik} \sin \theta_{ik} - B_{ik} \cos \theta_{ik}) \quad i \in \mathcal{N}$$
 (3)

$$q_i^{\min} \leq q_i^{\inf} \leq q_i^{\max}$$
 $i \in \mathcal{N}_G$ (4a)

$$v_i^{\min} \leq v_i \leq v_i^{\max}$$
 $i \in \mathcal{N}_{pq}$ (4b)

$$\varphi_l^{\min} \le \theta_l^{\mathrm{f}} - \theta_l^{\mathrm{t}} \le \varphi_l^{\max}$$
 $l \in \mathcal{E}$ (4c)

where $p_i^{\rm inj}$ and $q_i^{\rm inj}$ are the active and reactive power injection, and θ_i and v_i are the phase angle and voltage magnitude at bus i. The variable $\theta_{ik}=\theta_i-\theta_k$ represents the phase angle difference between bus i and k. Alternatively, the angle difference can be represented by $\theta_l^{\rm f}-\theta_l^{\rm t}$ where $\theta_l^{\rm f}$ and $\theta_l^{\rm t}$ denote the phase angle at from and to bus of the transmission line l. The operational constraints considered here are reactive power limits and voltage magnitude limits at the generators and phase angle difference limits on transmission lines.

In the steady-state analysis of power grids, the system operator has control over the generators, which is denoted by u.

In this article, the feasibility of active power injection at non-slack buses will be considered so that $u=p_{\rm ns}^{\rm inj}$. The reactive power injection at the PQ buses and voltage magnitude at the PV buses are assumed to be fixed to constant values although the framework can be extended to include them. The corresponding internal states are $x=\left[\theta_{\rm ns}^T\ v_{\rm pq}^T\right]^T$. The system operators need to set the control variable subject to the power flow feasibility set in (3) and (4). Our objective is to find a non-conservative subset around some known base operating point. The base operating point in Assumption 1 can be naturally chosen as the current operating point. This implies that

- 1) the system is operating at a normal condition where the operational constraints are respected, and
- 2) the system is not operating at the solvability boundary of the power flow equation.

Assumption 2 is naturally satisfied for the power flow equations because it can be decomposed by the nonlinearity involved in transmission lines and the shunt elements. The basis functions can be chosen to be $v_i v_k \cos(\theta_{ik})$ and $v_i v_k \sin(\theta_{ik})$ for each transmission line and the voltage magnitude squares. Since the electric grid is a sparsely connected network, the number of basis functions grows proportionally with respect to the number of buses and number of transmission lines.

C. Fixed Point Representation

The power flow equations can be converted into an equivalent fixed point form inspired by the Newton–Raphson method. Let us define the residues of basis functions around the nominal operating point as

$$g(x,u) = \psi(x,u) - J_{\psi,0}x$$
 (5)

where $J_{\psi,0} = \nabla_x \psi(x, u_0)|_{x=x_0}$. Note that the power flow Jacobian is a linear transformation of the basis function Jacobian (i.e., $J_{f,0} = MJ_{\psi,0}$). The equality constraint can be written as

$$f(x,u) = J_{f,0}x + Mg(x,u)$$
 (6)

where the first term is the linearization of the equation and the second term is the higher order residual. From Assumption 1, the power flow Jacobian is invertable, and the equality constraint can be written in the following fixed point form:

$$x = -J_{f,0}^{-1} Mg(x, u). (7)$$

The fixed point condition in (7) is an equivalent constraint to the equality condition in (1a).

Remark 2: The fixed point form in (7) is in the same form as a single iteration of Newton–Raphson method [29].

The Newton-Raphson method is one of the most popular algorithms for solving nonlinear equations including steady-state power flow equations [30]. It is widely used in practice due to its fast convergence to the solution given a good initial guess.

III. DERIVATION OF CONVEX RESTRICTION

In this section, we describe the procedure for constructing the convex restriction of given equality and inequality constraints.

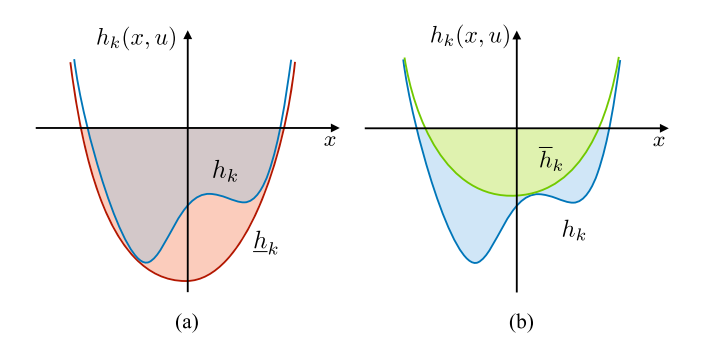


Fig. 2. Blue region is the epigraph of $h_k(x,u)$ that satisfies the inequality constraint: (a) shows the convex relaxation in red and (b) shows the convex restriction in green using envelopes.

A. Convex Restriction of Inequality Constraints

First, let us consider the convex restriction of inequality constraints and ignore equality constraints. This case is much more straightforward than the convex restriction with equality constraints. Suppose that a vector of functions $\overline{h}(x,u)$ and $\underline{h}(x,u)$ establishes bounds on h(x,u) such that

$$\underline{h}_k(x,u) \le h_k(x,u) \le \overline{h}_k(x,u). \tag{8}$$

The functions $\underline{h}_k(x,u)$ and $\overline{h}_k(x,u)$ are referred to as the under-estimator and over-estimator of $h_k(x,u)$, respectively. The following lemma shows an interesting comparison between the convex restriction and convex relaxation of inequality constraints.

Lemma 1: Suppose that under- and over-estimators $\underline{h}_k(x,u)$ and $\overline{h}_k(x,u)$ are convex functions. If (x,u) is feasible for $h(x,u) \leq 0$, then

$$h(x,u) < 0 \tag{9}$$

and the above condition forms the convex relaxation of the feasibility set. If

$$\overline{h}(x,u) \le 0 \tag{10}$$

then (x, u) is feasible for $h(x, u) \le 0$, and the above condition forms the convex restriction of the feasibility set.

Lemma 1 shows a simple contrast between the relaxation and restriction, and Fig. 2 graphically illustrates their differences. In this article, *convex envelope* refers to the convex over-estimator and concave under-estimator, and *concave envelope* refers to the concave over-estimator and convex underestimator. Examples of these envelopes are shown in Fig. 3. The convex envelope encloses a convex region, and it is widely used in convex relaxations of nonconvex optimization problems [7], [31]. As was shown in Lemma 1, it turns out that concave envelopes are necessary for constructing convex restrictions of inequality constraints. Later, we will show that even for the restriction of nonlinear equality constraints, concave envelopes need to be used to enforce convexity to the inner approximation.

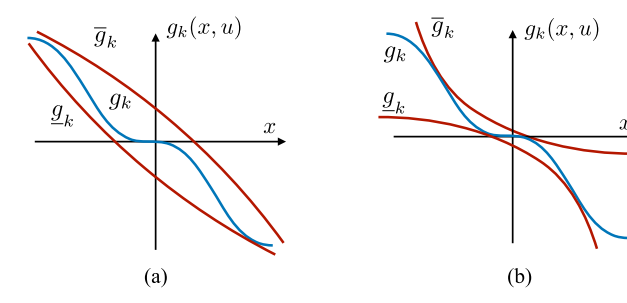


Fig. 3. Illustrations of (a) the convex envelope and (b) the concave envelope.

B. Preliminaries for Convex Restriction of Equality Constraints

In this section, the convex restriction of equality constraints will be presented. The derivation relies on Brouwer's fixed point theorem, which provides a sufficient condition for the solvability of the equality constraint. Given the fixed point equation in (7), the theorem states the following.

Theorem 1. (Brouwer's Fixed Point Theorem): Let $G: \mathcal{P} \to \mathcal{P}$ be a continuous map where \mathcal{P} is a compact and convex set in \mathbb{R}^n . Then the map has a fixed point in \mathcal{P} , namely, x = G(x) has a solution in $x \in \mathcal{P}$.

Brouwer's fixed point theorem provides a sufficient condition for the existence of a solution in the internal states. The control variables u can be considered as external parameters changing the fixed point equation in (7), which leads to the following lemma

Lemma 2: If $-J_{f,0}^{-1}Mg(x,u) \in \mathcal{P}$ for all $x \in \mathcal{P}$, then u is solvable and has at least one solution in $x \in \mathcal{P}$.

Proof: Let $G(x) = -J_{f,0}^{-1}Mg(x,u)$. Then, there exist a solution $x \in \mathcal{P}$ from Brouwer's fixed point theorem.

The existence of any self-mapping set guarantees the existence of a state solution, and the self-mapping set is not unique. This suggests the idea of proposing a class of convex and compact sets parametrized by some variable denoted by $b \in \mathbf{R}^p$. Instead of finding a single self-mapping set, a class of sets can be used to check Brouwer's self-mapping condition, and the solvability region will be the union of all control variables that have a self-mapping set in the state space. The self-mapping set will be denoted by $\mathcal{P}(b)$ to show that it is parametrized by b. Then, the existence of b such that $-J_{f,0}^{-1}Mg(\mathcal{P}(b),u)\subseteq\mathcal{P}(b)$ is sufficient for the Brouwer's self-mapping condition. This idea can be interpreted as lifting the optimization variables to include an additional variable b where the construction of convex restriction is less conservative.

C. Self-Mapping With Polytopes

While the self-mapping set can be any convex and compact set, a polytope will be considered in this article. There is a significant computational advantage of using a polytope because the set is described by inequality constraints involving just linear transformations. Let us consider a nonempty compact polytope

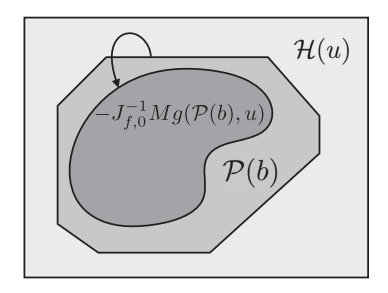


Fig. 4. Self-mapping in the domain of $\mathcal X$ is illustrated. Here, $\mathcal H(u)=\{x\mid h(x,u)\leq 0\}$, and the existence of the self-mapping set $\mathcal P(b)$ ensures solvability and feasibility of u.

set \mathcal{P}

$$\mathcal{P}(b) = \{ x \mid Ax \le b \} \tag{11}$$

where $A \in \mathbf{R}^{p \times n}$ is a constant matrix, and $b \in \mathbf{R}^p$ is a vector of variables. The matrix A is chosen such that it forms intervals that bound the nonlinearity involved in the basis functions. For example, $\sin(\theta^{\mathrm{f}} - \theta^{\mathrm{t}})$ can be effectively bounded by choosing A to be the incidence matrix. When the angle difference $\theta^{\mathrm{f}} - \theta^{\mathrm{t}} = E^T \theta$ has tight upper and lower bounds, the term $\sin(\theta^{\mathrm{f}} - \theta^{\mathrm{t}})$ can also be tightly bounded. By fixing A to be a constant matrix, the linear transformation does not introduce any extra complexity.

Lemma 2 provides a sufficient condition for the existence of internal states in $\mathcal{P}(b)$. The condition can be extended to include inequality constraints by ensuring the self-mapping set resides inside the inequality constraints. If $h(u,x) \leq 0$ for all $x \in \mathcal{P}(b)$, the existing internal state solution should also satisfy $h(u,x) \leq 0$. The self-mapping condition and the feasibility condition are illustrated in Fig. 4, and these conditions are stated formally in the following lemma.

Lemma 3: If there exists $b \in \mathbf{R}^p$ such that

$$\forall x \in \mathcal{P}(b), \ -J_{f,0}^{-1}Mg(x,u) \in \mathcal{P}(b)$$
$$\forall x \in \mathcal{P}(b), \ h(x,u) \le 0$$
 (12)

then u is feasible and there exists a corresponding state solution that satisfies $x \in \mathcal{P}(b)$.

Proof: The first condition ensures the self-mapping under the map $x \to -J_{f,0}^{-1}Mg(x,u)$, and thus there exists $x \in \mathcal{P}(b)$ by Lemma 2. The second condition ensures that for all $x \in \mathcal{P}(b)$, $h(x,u) \leq 0$. The control variable u satisfies both constraints in (1a) and (1b), and thus belongs to the feasibility set.

Notice that these conditions are described as an intersection of two containment conditions on the self-mapping set. The self-mapping condition for solvability can be rewritten as the following condition.

Lemma 4: The control variable u is solvable and there exists a corresponding state solution that satisfies $x \in \mathcal{P}(b)$ if there exists some $b \in \mathbf{R}^p$ such that for all $i = 1, \ldots, p$

$$\max_{x \in \mathcal{P}(b)} K_i g(x, u) \le b \tag{13}$$

where $K_i \in \mathbf{R}^{1 \times q}$ is the *i*th row of the matrix K and

$$K = -AJ_{f,0}^{-1}M. (14)$$

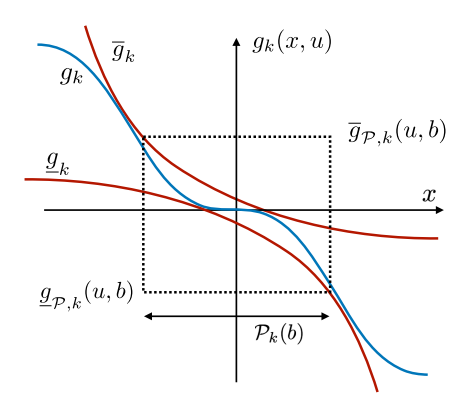


Fig. 5. Over- and under-estimators $\overline{g}_{\mathcal{P},k}(u,b)$ and $\underline{g}_{\mathcal{P},k}(u,b)$ provide the bound on g_k over the set $\mathcal{P}(b)$. The dashed box contains all the nonlinearity over \mathcal{P} . Note that the upper and lower bounds always occur at the extreme points when the concave envelopes are used.

Proof: The above condition is a sufficient condition to $-AJ_{f,0}^{-1}Mg(x,u) \leq b$ for all $x \in \mathcal{P}(b)$, which shows the self-mapping of the set $\mathcal{P}(b)$. Then, there exists a solution $x \in \mathcal{P}(b)$ from Lemma 3.

In the next section, we find the upper bound of the left-hand side of the inequality in (13) by using the concave envelopes.

D. Enclosure of Concave Envelope

Consider an over- and under-estimator of g(x,u), denoted by $\overline{g}(x,u)$ and g(x,u):

$$g_k(x,u) \le g_k(x,u) \le \overline{g}_k(x,u)$$
 (15)

where $\underline{g}_k(x,u)$ is concave, and $\overline{g}_k(x,u)$ is convex with respect to x and u. This is the concave envelope presented in Fig. 3. While the above envelope gives the bound for all x, the inequality condition in Lemma 4 requires the bound over the set $\mathcal{P}(b)$. Suppose that the domain of x is restricted to $\mathcal{P}(b)$, and let us establish the bound over the self-mapping set. These bounds are given by the following definition:

$$\overline{g}_{\mathcal{P},k}(u,b) = \max_{x \in \mathcal{P}(b)} \overline{g}_k(x,u)$$
 (16a)

$$\underline{g}_{\mathcal{P},k}(u,b) = \min_{x \in \mathcal{P}(b)} \underline{g}_k(x,u) \tag{16b}$$

and the following holds

$$g_{\mathcal{P},k}(u,b) \le g_k(x,u) \le \overline{g}_{\mathcal{P},k}(u,b), \quad \forall x \in \mathcal{P}(b).$$
 (17)

This forms a compact region that contains the nonlinearity in $\mathcal{P}(b)$ as illustrated in Fig. 5. The self-mapping set could be interpreted as an intersection of intervals in some transformed variables.

E. Enforcing Convexity by Vertex Tracking

This section introduces the vertex tracking, which is one of the key concepts that allow the scalable construction of convex restriction. Let us denote $\mathcal{P}_k(b)$ the polytope formed in the space of variables involved in $g_k(x,u)$. Then the interval bounds defined in (16) can be rewritten by the following lemma.

Lemma 5: Suppose that $\overline{g}_k(v,u)$ and $\underline{g}_k(v,u)$ are convex and concave functions. The interval bound $\overline{g}_{\mathcal{P},k}(u,b)$ and $\underline{g}_{\mathcal{P},k}(u,b)$ in (16) are also convex and concave in (u,b) and are given by

$$\overline{g}_{\mathcal{P},k}(u,b) = \max_{v \in \partial \mathcal{P}_k(b)} \overline{g}_k(v,u)$$
 (18a)

$$\underline{g}_{\mathcal{P},k}(u,b) = \min_{v \in \partial \mathcal{P}_k(b)} \underline{g}_k(v,u) \tag{18b}$$

where $\partial \mathcal{P}_k(b)$ denotes the vertices of polytope $\mathcal{P}_k(b)$.

Proof: Since $\overline{g}_k(v,u)$ is a convex function and $\mathcal{P}(b)$ is a convex set, its maximum always occurs at the extreme points. Moreover, (18a) is a point-wise maximum over all vertices, therefore the convexity is preserved with respect to both u and b [32]. The function $\underline{g}_k(v,u)$ can be proved in the same way.

Remark 3: Given Assumption 2, the number of variables involved in ψ_k is finite and independent of n and s, which are the number of constraints. Then, the number of vertices of $\mathcal{P}_k(b)$ is also finite independent of n and s.

Given the interval bound defined by (18), the convexity can be enforced to the self-mapping condition in Lemma 4. First, the positive and negative parts of matrix $K \in \mathbf{R}^{p \times q}$ are defined as $K^+, K^- \in \mathbf{R}^{p \times q}$ with

$$K_{ij}^{+} = \begin{cases} K_{ij} & \text{if } K_{ij} > 0 \\ 0 & \text{otherwise} \end{cases} \quad K_{ij}^{-} = \begin{cases} K_{ij} & \text{if } K_{ij} < 0 \\ 0 & \text{otherwise} \end{cases}$$

where K_{ij} refer to ith row and jth column of matrix K. Note $K = K^+ + K^-$ with $K^+_{ij} \geq 0$ and $K^-_{ij} \leq 0$. The next lemma provides a convex upper bound for left-hand side of (13) in Lemma 4.

Lemma 6: Given a matrix $K \in \mathbf{R}^{p \times q}$, the following inequality holds for $i = 1, \dots, p$

$$\max_{x \in \mathcal{P}(b)} K_i g(x, u) \le K_i^+ \overline{g}_{\mathcal{P}}(u, b) + K_i^- \underline{g}_{\mathcal{P}}(u, b)$$
 (20)

where the right-hand side of the equation is a convex function with respect to (u, b).

Proof: Since $\overline{g}_{\mathcal{P}}(u,b)$ and $\underline{g}_{\mathcal{P}}(u,b)$ are the upper and lower bounds on g(x,u)

$$\max_{x \in \mathcal{P}(b)} K_i g(x, u) \le \max_{x \in \mathcal{P}(b)} [K_i^+ \overline{g}(u, b) + K_i^- \underline{g}(u, b)]$$
$$\le K_i^+ \max_{x \in \mathcal{P}(b)} \overline{g}(u, b) + K_i^- \min_{x \in \mathcal{P}(b)} \underline{g}(u, b)$$

for all $x \in \mathcal{P}(b)$. Moreover, $\overline{g}_{\mathcal{P}}(u,b)$ and $-\underline{g}_{\mathcal{P}}(u,b)$ are convex and concave functions from Lemma 5, and K^+ and K^- have nonnegative entries. Therefore, the convexity is preserved to the right-hand side of (20) [32].

Lemma 6 provides a convex over-estimator of the self-mapping condition. Let us first consider only the equality constraint in (1a). The following theorem provides the convex restriction of solvability sets.

Theorem 2: Given a nonlinear equality constraint in (1a), u is solvable if there exists $b \in \mathbb{R}^p$ such that

$$K^{+}\overline{g}_{\mathcal{P}}(u,b) + K^{-}g_{\mathcal{P}}(u,b) \le b. \tag{21}$$

Moreover, the corresponding state variable is $x \in \mathcal{P}(b)$.

Proof: From Lemma 6

$$\max_{x \in \mathcal{P}(b)} Kg(x, u) \le K^{+} \overline{g}_{\mathcal{P}}(u, b) + K^{-} \underline{g}_{\mathcal{P}}(u, b) \le b.$$

Thus $\max_{x \in \mathcal{P}(b)} Kg(x, u) \leq b$, and u is solvable with $x \in \mathcal{P}(b)$ from Lemma 4. \square

In order to incorporate inequality constraints, let us define the bound on $\psi(x,u)$ using Lemma 5

$$\overline{\psi}_{\mathcal{P},k}(u,b) = \max_{v \in \partial \mathcal{P}_k(b)} \overline{\psi}_k(v,u)$$
 (22a)

$$\underline{\psi}_{\mathcal{P},k}(u,b) = \min_{v \in \partial \mathcal{P}_k(b)} \underline{\psi}_k(v,u). \tag{22b}$$

A convex sufficient condition for $h_k(x,u) \leq 0$ for all $x \in \mathcal{P}_k(b)$ can be derived using Lemma 6. This ensures that the self-mapping set is contained in the feasibility set for the inequality constraints (i.e., $\mathcal{P}(b) \subseteq \mathcal{H}(u)$). The following theorem provides the convex restriction of the feasibility set, which is the main result in this article.

Theorem 3. (Convex Restriction): Given nonlinear equality and inequality constraints in (1a) and (1b), u is feasible if there exists $b \in \mathbb{R}^p$ such that

$$K^{+}\overline{g}_{\mathcal{P}}(u,b) + K^{-}\underline{g}_{\mathcal{P}}(u,b) \leq b$$

$$L^{+}\overline{\psi}_{\mathcal{P}}(u,b) + L^{-}\psi_{\mathcal{P}}(u,b) \leq 0.$$
(23)

Proof: The inequality condition $K^+ \overline{g}_{\mathcal{P}}(u,b) + K^- \underline{g}_{\mathcal{P}}(u,b) \leq b$ ensures the existence of the state solution according to Theorem 2. The second condition ensures that the polytope $\mathcal{P}(b)$ lies within the feasible region of inequality constraint. That is, for $i=1,\ldots,s$

$$\max_{x \in \mathcal{P}(b)} L_i \psi(x, u) \le L_i^+ \overline{\psi}_{\mathcal{P}}(u, b) + L_i^- \underline{\psi}_{\mathcal{P}}(u, b) \le 0.$$

Therefore, this is a sufficient condition for the solvability of (1a) and the feasibility of (1b).

Note that the left-hand side functions in inequalities (23) are convex functions as shown in Lemma 6. Therefore, (23) provides a convex sufficient convex condition for feasibility, which was the objective of the convex restriction. Moreover, the convex restriction is guaranteed to be nonempty given a feasible base point stated in Assumption 1.

Remark 4: If $\overline{g}_i(x_0, u_0) = \underline{g}_i(x_0, u_0)$, and $\overline{\psi}_i(x_0, u_0) = \underline{\psi}(x_0, u_0)$ (i.e., the concave envelopes are tight and feasible at the base point), then the convex restriction in (23) is nonempty and contains the base point.

Proof: Since $\mathcal{P}(b) = \{x \mid Ax \leq b\}$ is closed, there exists b such that $\mathcal{P}(\hat{b}) = \{x_0\}$. Given that the concave envelopes are tight at the base point and the base point is feasible (Assumption 1), it follows

$$K^{+}\overline{g}_{\mathcal{P}}(u_{0},\hat{b}) + K^{-}\underline{g}_{\mathcal{P}}(u_{0},\hat{b}) = Kg(x_{0},u_{0}) = \hat{b}$$

$$L^{+}\overline{\psi}_{\mathcal{P}}(u_{0},\hat{b}) + L^{-}\underline{\psi}_{\mathcal{P}}(u_{0},\hat{b}) = L\psi(x_{0},u_{0}) \leq 0.$$

The condition in Theorem 3 is always satisfied at the base point, and thus the convex restriction contains the base point and is nonempty.

From Remark 4, we can always construct a nonempty convex restriction around a feasible base point. The current or planned operating point can be naturally used as the base point for power flow feasibility set, which is given to the system operators through measurements. By changing the base point, the convex restriction can be constructed at an arbitrary location in the feasibility set.

IV. CONVEX RESTRICTION OF POWER FLOW FEASIBILITY SET

In this section, the convex restriction is constructed for the ac power flow equations in polar coordinates. The polar representation includes the voltage magnitudes explicitly in the equation, and it is convenient to enforce the voltage magnitude and phase angle limits. The ac power flow equations in (3) can be written in the complex plane for all $i \in \mathcal{N}$

$$p_i^{\text{inj}} + jq_i^{\text{inj}} = \sum_{k \in \mathcal{N}} Y_{ik}^H v_i v_k e^{-j\theta_{ik}}$$

where $Y_{ik} = G_{ik} + jB_{ik}$, and Y_{ik}^H is the conjugate of Y_{ik} . Suppose that the feasible base point has the state θ_0 and v_0 , then

$$p_i^{\mathrm{inj}} + jq_i^{\mathrm{inj}} = \sum_{k \in \mathcal{N}} \left(Y_{ik}^H e^{-j\theta_{0,ik}} \right) v_i v_k e^{-j(\theta_{ik} - \theta_{0,ik})} \quad i \in \mathcal{N}$$

where the base point phase is combined with the admittance matrix. Then, the phase-adjusted admittance matrix can be defined as $\widetilde{G}_{ik}+j\widetilde{B}_{ik}=Y_{ik}^He^{-j\theta_{0,ik}}$. Let us define the difference in angle as $\varphi=E^T\theta$ and $\widetilde{\varphi}=E^T\theta-E^T\theta_0$ where E is the incidence matrix of the network. The power flow equations can be rewritten for $i\in\mathcal{N}_{\mathrm{ns}}$ for active power and $i\in\mathcal{N}_{\mathrm{pv}}$ for reactive power as follows:

$$p_{i}^{\text{inj}} = \sum_{l \in \mathcal{E}} v_{l}^{\text{f}} v_{l}^{\text{t}} (\hat{G}_{ik}^{c} \cos \tilde{\varphi}_{l} + \hat{B}_{ik}^{s} \sin \tilde{\varphi}_{l}) + G_{ii} v_{i}^{2}$$

$$q_{i}^{\text{inj}} = \sum_{l \in \mathcal{E}} v_{l}^{\text{f}} v_{l}^{\text{t}} (\hat{G}_{ik}^{c} \sin \tilde{\varphi}_{l} - \hat{B}_{ik}^{s} \cos \tilde{\varphi}_{l}) - B_{ii} v_{i}^{2}$$

$$(24)$$

where $v^f \in \mathbf{R}^{|\mathcal{E}|}$ and $v^t \in \mathbf{R}^{|\mathcal{E}|}$ are voltage magnitudes at the *from* and *to* bus of transmission lines. The constant matrices \widehat{G}^c , $\widehat{G}^s \in \mathbf{R}^{|\mathcal{N}| \times |\mathcal{E}|}$ are defined as

$$\widehat{G}_{kl}^{c} = \begin{cases} \widetilde{G}_{ik} & \text{if } i = l^{\text{f}} \\ \widetilde{G}_{ki} & \text{if } i = l^{\text{t}} & \widehat{G}_{kl}^{s} = \begin{cases} \widetilde{G}_{ik} & \text{if } i = l^{\text{f}} \\ -\widetilde{G}_{ki} & \text{if } i = l^{\text{t}} \end{cases}$$
 (25)

where $l^{\rm f}$ and $l^{\rm t}$ are the from and to bus of the transmission line l. The matrices \widehat{B}^c , $\widehat{B}^s \in \mathbf{R}^{|\mathcal{N}| \times |\mathcal{E}|}$ are defined in the same way by simply replacing the letter G by B.

The advantage of using (24) over (3) is that the concave envelope over the trigonometric function can be systematically derived while ensuring zero gap between over- and under-estimator at the base point. From the power flow equations, basis functions

are chosen to be

$$\psi(x, u) = \begin{bmatrix} p_{\text{ns}}^{\text{inj}} \\ q_{\text{pq}}^{\text{inj}} \\ v^{\text{f}} v^{\text{t}} \cos \tilde{\varphi} \\ v^{\text{f}} v^{\text{t}} \sin \tilde{\varphi} \\ v^{2} \end{bmatrix}$$
 (26)

where $p_{\rm ns}^{\rm inj}$ is the set of active power injections at nonslack buses, and $q_{\rm pq}^{\rm inj}$ is the set of reactive power injections at the PQ buses. With the given basis functions, the equality constraint is $f(x,u)=M\psi(x,u)=0$ with

$$M = \begin{bmatrix} I & \mathbf{0} & -\widehat{G}_{\text{ns}}^c & -\widehat{B}_{\text{ns}}^s & -G_{\text{ns}}^d \\ \mathbf{0} & I & \widehat{B}_{\text{pq}}^c & -\widehat{G}_{\text{pq}}^s & B_{\text{pq}}^d \end{bmatrix}$$
(27)

where I and $\mathbf{0}$ are an identity matrix and a zero matrix with appropriate sizes. The matrices G^d and B^d are diagonal matrices with its diagonal elements equal to the diagonals of G and B, respectively. The matrix $\widehat{G}^c_{\rm ns}$ denotes a matrix with only nonslack bus rows from \widetilde{G}^c , and $\widehat{G}^c_{\rm pq}$ denotes a matrix with only the PQ bus rows from \widetilde{G}^c . The matrices $\widehat{B}^c_{\rm ns}$ and $\widehat{B}^c_{\rm pq}$ are built in the same way. Given the basis functions in (26), its residues can be computed using (5)

$$g(x,u) = \begin{bmatrix} p_{\text{ns}}^{\text{inj}} \\ q_{\text{pq}}^{\text{inj}} \\ v^{\text{f}}v^{\text{t}}\cos\tilde{\varphi} - v_{0}^{\text{f}}v^{\text{t}} - v^{\text{f}}v_{0}^{\text{t}} \\ v^{\text{f}}v^{\text{t}}\sin\tilde{\varphi} - v_{0}^{\text{f}}v_{0}^{\text{t}}\varphi \\ v^{2} - 2v_{0}v \end{bmatrix}$$
(28)

where the omitted product is overloaded to an element-wise product. For example, $v^{\rm f}v^{\rm t}\cos\varphi$ is an element-wise product of $v^{\rm f}, v^{\rm t}$, and $\cos\varphi$. Here, we note that the maximum number of variables associated with each basis function is four, which are voltage magnitudes and phase angles at *from* and *to* bus of the associated transmission line. The self-mapping polytope is chosen as $\mathcal{P} = \{x \mid Ax \leq b\}$ where

$$A = \begin{bmatrix} E_{\text{ns}}^{T} & \mathbf{0} \\ \mathbf{0} & I \\ -E_{\text{ns}}^{T} & \mathbf{0} \\ \mathbf{0} & -I \end{bmatrix} \text{ and } b = \begin{bmatrix} \overline{\varphi} \\ \overline{v}_{\text{pq}} \\ -\underline{\varphi}^{\text{min}} \\ -v_{\text{ng}} \end{bmatrix}$$
(29)

and $E_{\rm ns}$ is the incidence matrix with the rows chosen for only nonslack buses. By choosing A as the above, we can interpret b as the upper and lower bounds of φ and $v_{\rm pq}$. The operational constraints on the voltage magnitudes and phase angles can be written as $Ax \leq b^{\rm max}$ where

$$b^{\max} = \left[\varphi^{\max^T} \ v_{pq}^{\max T} \ - \varphi^{\min T} \ - v_{pq}^{\min T} \right]^T. \tag{30}$$

The reactive power limits on PV buses can be written as $L\psi(x,u) \leq d$ where

$$L = \begin{bmatrix} \mathbf{0} & \mathbf{0} & -\widehat{B}_{\text{pv}}^c & \widehat{G}_{\text{pv}}^s & -\widehat{B}_{\text{pv}}^d \\ \mathbf{0} & \mathbf{0} & \widehat{B}_{\text{pv}}^c & -\widehat{G}_{\text{pv}}^s & \widehat{B}_{\text{pv}}^d \end{bmatrix}, \quad d = \begin{bmatrix} q_{\text{pq}}^{\text{max}} \\ -q_{\text{pq}}^{\text{min}} \end{bmatrix}.$$
(31)

The inequality constrained set is then $\mathcal{H}(u) = \{x \mid Ax \leq b^{\max}, \ L\psi(x,u) \leq d\}$. The self-mapping set belongs to the inequality constrained set (i.e., $\mathcal{P} \subseteq \mathcal{H}(u)$) if $b \leq b^{\max}$ and $L^+\overline{\psi}(u,b) + L^-\underline{\psi}(u,b) \leq d$. The trigonometric terms and its product with voltage magnitudes are bounded effectively by the phase angle differences and voltage magnitudes. In the next section, quadratic concave envelopes will be derived for bilinear and trigonometric functions, and the convex restriction will be constructed with convex quadratic constraints.

A. Quadratic Concave Envelopes

The main nonlinearities involved in the power flow equations in polar coordinates are the quadratic, trilinear, and trigonometric functions. Following corollaries provide concave envelopes for commonly used functions that can be used as the building blocks for bounding more complicated functions.

Corollary 1: Unitary quadratic functions can be bounded by the following concave envelopes with the base point at x_0

$$x^{2} \ge 2x - x_{0}^{2}$$

$$x^{2} < x^{2}.$$
(32)

Corollary 2: Bilinear functions can be bounded by the following concave envelopes with some ρ_1 , $\rho_2 > 0$ and the base point x_0 , y_0

$$xy \ge -\frac{1}{4} \left[\rho_1 \left(x - x_0 \right) - \frac{1}{\rho_1} \left(y - y_0 \right) \right]^2$$

$$+ x_0 y + x y_0 - x_0 y_0$$

$$xy \le \frac{1}{4} \left[\rho_2 \left(x - x_0 \right) + \frac{1}{\rho_2} \left(y - y_0 \right) \right]^2$$

$$+ x_0 y + x y_0 - x_0 y_0.$$

$$(33)$$

The over-estimator is tight along $\rho_2(x-x_0)-\frac{1}{\rho_2}(y-y_0)=0$, and the under-estimator is tight along $\rho_2(x-x_0)+\frac{1}{\rho_2}(y-y_0)=0$. Both the over- and under-estimators are tight at the base point, (x_0,y_0) .

Corollary 3: Trigonometric functions can be bounded by the following quadratic concave envelopes for all $\theta^{\max} \in [0, \pi]$ and $\theta^{\min} \in [-\pi, 0]$

$$\sin \theta \ge \theta + \left(\frac{\sin \theta^{\max} - \theta^{\max}}{(\theta^{\max})^2}\right) \theta^2, \ \theta < \theta^{\max}$$

$$\sin \theta \le \theta + \left(\frac{\sin \theta^{\min} - \theta^{\min}}{(\theta^{\min})^2}\right) \theta^2, \ \theta > \theta^{\min}$$
(34)

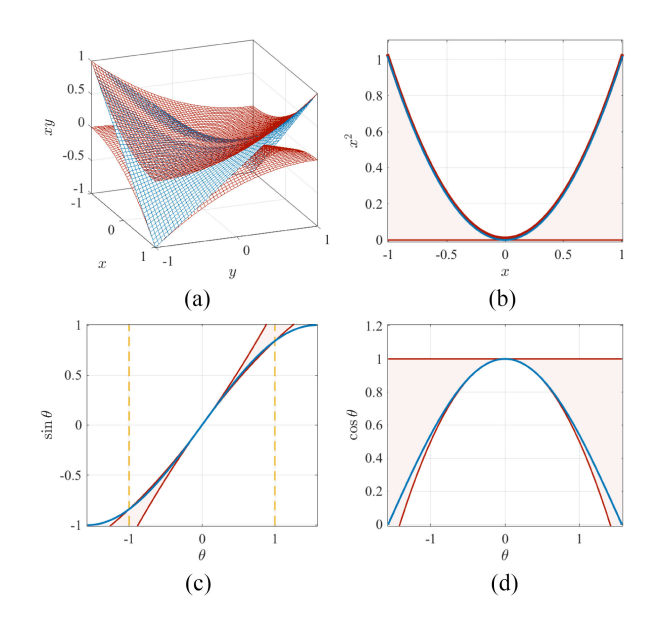


Fig. 6. Illustrations of concave envelopes of a (a) bilinear, (b) unitary quadratic, (c) sine, and (d) cosine functions. In (c), θ^{\max} and θ^{\min} are marked with yellow dashed lines.

and for all θ

$$\cos \theta \ge 1 - \frac{1}{2}\theta^2$$

$$\cos \theta < 1.$$
(35)

Envelopes for unitary quadratic, bilinear and trigonometric functions are illustrated in Fig. 6. More complicated functions, such as trilinear functions can be bounded by cascading bilinear concave envelope. For example, the term $v_l^t v_l^t \cos \tilde{\varphi}_l$ can bounded by defining an intermediate variable $vv_l = v_l^t v_l^t$, and the bilinear envelope can be applied to vv_l and $\cos \tilde{\varphi}_l$. In the following corollary, we finally state the analytical expression of the convex restriction of the power flow feasibility set.

Corollary 4. (QC Restriction of Power Flow Equations with Operational Constraints): The control variable $u=p_{\rm ns}$ has at least one internal state solution, $x=\left[\theta_{\rm ns}^T\ v_{\rm pq}^T\right]^T$ satisfying power flow equations in (3) and operational constraints in (4) if there exists $b\in {\bf R}^p$ such that

$$K^{+}\overline{g}_{\mathcal{P}} + K^{-}\underline{g}_{\mathcal{P}} \leq b$$

$$L^{+}\overline{\psi}_{\mathcal{P}} + L^{-}\psi_{\mathcal{P}} \leq d, \quad b \leq b^{\max}$$
(36)

where

$$b = \begin{bmatrix} \overline{\varphi}^T & \overline{v}_{pq}^T & -\underline{\varphi}^T & -\underline{v}_{pq}^T \end{bmatrix}^T$$

$$\overline{g}_{\mathcal{P}} = \begin{bmatrix} p_{ns}^T & q_{pq}^T & \overline{g}_{\mathcal{P}}^{C^T} & \overline{g}_{\mathcal{P}}^{S^T} & \overline{g}_{\mathcal{P}}^{Q^T} \end{bmatrix}^T$$

$$\underline{g}_{\mathcal{P}} = \begin{bmatrix} p_{ns}^T & q_{pq}^T & \underline{g}_{\mathcal{P}}^{C^T} & \underline{g}_{\mathcal{P}}^{S^T} & \underline{g}_{\mathcal{P}}^{Q^T} \end{bmatrix}^T$$

$$\overline{\psi}_{\mathcal{P}} = \begin{bmatrix} p_{ns}^T & q_{pq}^T & \overline{\psi}_{\mathcal{P}}^{C^T} & \overline{\psi}_{\mathcal{P}}^{S^T} & \overline{\psi}_{\mathcal{P}}^{Q^T} \end{bmatrix}^T$$

$$\underline{\psi}_{\mathcal{P}} = \begin{bmatrix} p_{ns}^T & q_{pq}^T & \underline{\psi}_{\mathcal{P}}^{C^T} & \underline{\psi}_{\mathcal{P}}^{S^T} & \underline{\psi}_{\mathcal{P}}^{Q^T} \end{bmatrix}^T$$

$$\underline{\psi}_{\mathcal{P}} = \begin{bmatrix} p_{ns}^T & q_{pq}^T & \underline{\psi}_{\mathcal{P}}^{C^T} & \underline{\psi}_{\mathcal{P}}^{S^T} & \underline{\psi}_{\mathcal{P}}^{Q^T} \end{bmatrix}^T.$$

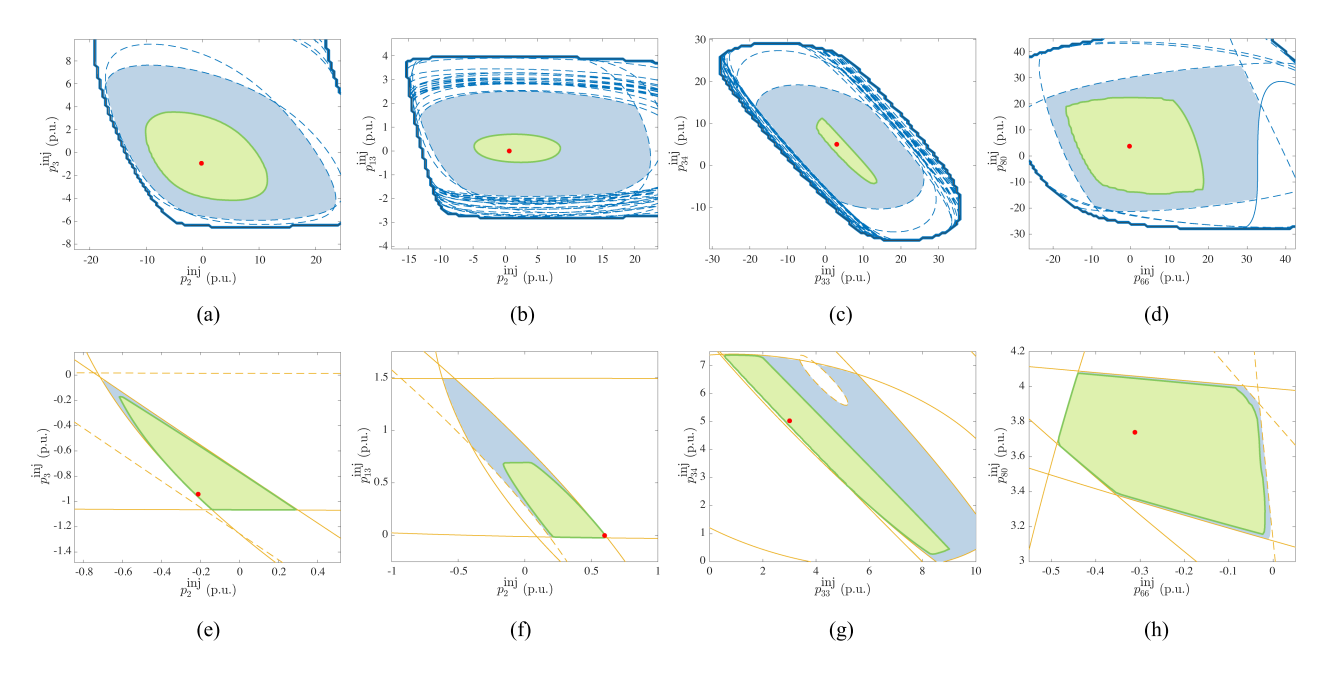


Fig. 7. Top four figures show the convex restrictions of feasible active power injection sets in the (a) 14-bus, (b) 30-bus, (c) 39-bus, and (d) 118-bus systems with voltage magnitude limits. The bottom four figures show the convex restrictions of the feasible active power injection sets in the (e) 14-bus, (f) 30-bus, (g) 39-bus, and (h) 118-bus with voltage magnitude and reactive power injection limits. Thick blue lines show the solvability boundary. Blue lines and yellow lines show voltage magnitude and reactive power injection limits with its upper limits in solid lines and its lower limits in dashed lines.

Variables $g_{\mathcal{P},l}^C$, $g_{\mathcal{P},l}^S$, and $g_{\mathcal{P},l}^Q$ with overlines and underlines denote the variables representing interval bounds of nonlinear elements in (28). Their explicit bounds are provided in the appendix.

Remark 5: The number of constraints grows linearly with respect to the number of buses and the number of lines. The number of constraints involved in Corollary 4 is less than $a|\mathcal{N}| + b|\mathcal{E}|$ where $|\mathcal{N}|$ and $|\mathcal{E}|$ are the number of buses and transmission lines, and a and b are constants independent of the system size.

B. Visualization of Convex Restrictions

This section provides a visualization of the convex restriction in two-dimensional space where the constraints were implemented in JuMP/Julia [33]. The plots were drawn by varying two control variables and fixing all other control variables. This creates a cross-section plot of the feasibility set that cuts through the base point. The actual feasible set was solved using the Newton–Raphson method with MATPOWER, and the same data set was used for convex restriction [28].

Fig. 8 shows the convex restriction of the modified 9-bus system. The voltage magnitude limits were set to 1% deviation from the base point in order to create a clear nonconvexity in the plot. The convex restriction was plotted by testing the feasibility of the constraint by checking violation of any operational limits. Fig. 7 shows test results in a larger system for IEEE 14-bus, 30-bus, 39-bus, and 118-bus systems. The operational limits were provided in pglib library v19.01 without any modification. The results show that the convex restriction is tight along some of the boundaries compared to the true feasibility set.

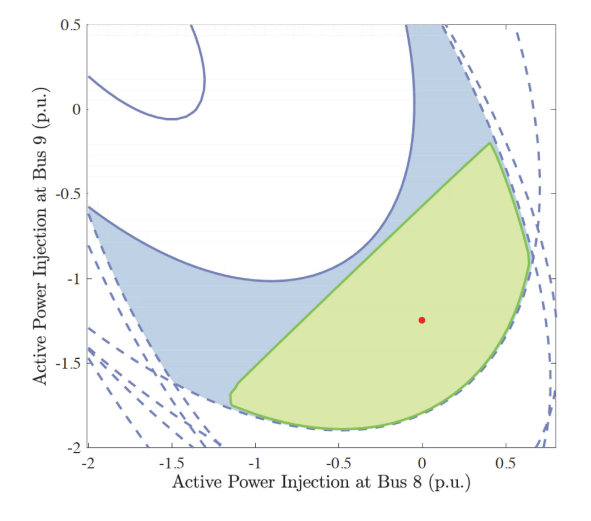


Fig. 8. Convex restriction of feasible active power injection set in a 9-bus system with the voltage limit of 1% deviation from the base operating point. The red dot denotes the base point. Solid blue lines show the voltage magnitude upper limits and dashed blue lines show the voltage magnitude lower limits.

V. CONCLUSION

This article proposed the convex restriction of a general feasibility set and presented its application to the power flow equations with operational constraints. These results give new insights and understandings of power flow feasibility sets as a counterpart to the convex relaxation. The convex restriction of power flow feasibility sets was constructed in a closed-form expression with convex quadratic constraints. The reliability of

the power grid is the top priority in the operation and analysis, and the convex restriction gives a guarantee for a steady-state solution that respects operational constraints. Cross-section plots of the convex restriction in IEEE test cases showed that our construction is very close to the true feasible region along some of the boundaries. For future work, our closed-form expression can replace the power flow equations to design tractable algorithms for the OPF proem and the steady-state security assessment.

APPENDIX

The bounds over the self-mapping set used in the convex restriction of power flow feasibility sets are listed here. The self-mapping set forms an intersection of intervals given by $\varphi_l \in [\underline{\varphi}_l, \overline{\varphi}_l]$ and $v_i \in [\underline{v}_i, \overline{v}_i]$ for all $l \in \mathcal{E}$ and $i \in \mathcal{N}$. These are results directly from Lemma 5 with envelopes presented in Corollary 1, 2, and 3. The constants $\rho_1 = 1$ and $\rho_2 = 1$ were used for bounding bilinear functions.

A. Interval Bounds for Cosine Function

The function $g_l^{\cos} = \cos \tilde{\varphi}_l - 1$ over $\varphi_l \in [\underline{\varphi}_l, \overline{\varphi}_l]$ is bounded by the following inequalities for all $l \in \mathcal{E}$:

$$\overline{g}_l^{\cos} \ge 0, \ \underline{g}_l^{\cos} \le -\frac{(\varphi_{i,l} - \varphi_{0,l})^2}{2}$$

where $\varphi_{i,l} \in {\overline{\varphi}_l, \underline{\varphi}_l}$.

B. Interval Bounds for Sine Function

Assuming $\overline{\varphi} \in [0, \pi]$ and $\underline{\varphi} \in [-\pi, 0]$, $g_l^{\sin} = \sin \tilde{\varphi}_l$ over $\varphi_l \in [\underline{\varphi}_l, \overline{\varphi}_l]$ is bounded by the following inequalities for all $l \in \mathcal{E}$:

$$\begin{split} & \overline{g}_{i,l}^{\sin} \geq \left(\varphi_{i,l} - \varphi_{0,l}\right) + \left(\frac{\sin \varphi_l^{\min} - \varphi_l^{\min}}{(\varphi_l^{\min})^2}\right) \left(\varphi_{i,l} - \varphi_{0,l}\right)^2 \\ & \underline{g}_{i,l}^{\sin} \leq \left(\varphi_{i,l} - \varphi_{0,l}\right) + \left(\frac{\sin \underline{\varphi}_l^{\max} - \underline{\varphi}_l^{\max}}{(\underline{\varphi}_l^{\max})^2}\right) \left(\varphi_{i,l} - \varphi_{0,l}\right)^2 \\ & \underline{\varphi}_l \leq \underline{\varphi}_l^{\max}, \ \ \overline{\varphi}_l \geq \overline{\varphi}_l^{\min} \end{split}$$

where $\varphi_{i,l} \in \{\overline{\varphi}_l, \varphi_l\}$.

C. Interval Bounds for Bilinear Function

The function $g^{vv} = v_l^f v_l^t - v_{0,l}^f v_{0,l}^t$ over $v_i \in [\underline{v}_i, \overline{v}_i]$ is bounded by the following inequalities for all $l \in \mathcal{E}$:

$$\begin{split} \overline{g}_{j,l}^{vv} &\geq \frac{1}{4} \left(\Delta v_{j,l}^{\mathrm{f}} + \Delta v_{j,l}^{\mathrm{t}} \right)^{2} + v_{0,l}^{\mathrm{f}} \Delta v_{j,l}^{\mathrm{t}} + \Delta v_{j,l}^{\mathrm{f}} v_{0,l}^{\mathrm{t}} \\ \underline{g}_{j,l}^{vv} &\leq -\frac{1}{4} \left(\Delta v_{j,l}^{\mathrm{f}} - \Delta v_{j,l}^{\mathrm{t}} \right)^{2} + v_{0,l}^{\mathrm{f}} \Delta v_{j,l}^{\mathrm{t}} + \Delta v_{j,l}^{\mathrm{f}} v_{0,l}^{\mathrm{t}} \\ \underline{g}_{l}^{vv} &\leq \underline{g}_{j,l}^{vv}, \quad \overline{g}_{l}^{vv} \geq \overline{g}_{j,l}^{vv} \end{split}$$

for each $(v_{j,l}^{\mathrm{f}},\,v_{j,l}^{\mathrm{t}})\in\{(\overline{v}_l^{\mathrm{f}},\,\overline{v}_l^{\mathrm{t}}),\,(\overline{v}_l^{\mathrm{f}},\,\underline{v}_l^{\mathrm{t}}),\,(\underline{v}_l^{\mathrm{f}},\,\overline{v}_l^{\mathrm{t}}),\,(\underline{v}_l^{\mathrm{f}},\,\underline{v}_l^{\mathrm{t}})\}$ and $\Delta v_l=v_l-v_{0,l}$ denotes the difference respect to the base point.

D. Interval Bounds for $v^f v^t \cos \varphi$

The function $\psi^C = v^{\mathrm{f}} v^{\mathrm{t}} \cos \varphi$ and $g^C = v^{\mathrm{f}} v^{\mathrm{t}} \cos \varphi - v_0^{\mathrm{f}} v^{\mathrm{t}} - v^{\mathrm{f}} v_0^{\mathrm{t}}$ over $v_i \in [\underline{v}_i, \overline{v}_i]$ and $\varphi_l \in [\underline{\varphi}_l, \overline{\varphi}_l]$ are bounded by the following inequalities for all $l \in \mathcal{E}$:

$$\begin{split} \overline{\psi}_{\mathcal{P},l}^{C} &\geq \overline{g}_{j,l}^{vv} + v_{0,l}^{\mathrm{f}} v_{0,l}^{\mathrm{t}} \\ \underline{\psi}_{\mathcal{P},l}^{C} &\leq -\frac{1}{4} (g_{j,l}^{vv} - g_{l}^{\cos})^{2} + v_{0,l}^{\mathrm{f}} v_{0,l}^{\mathrm{t}} g_{l}^{\cos} + g_{j,l}^{vv} + v_{0,l}^{\mathrm{f}} v_{0,l}^{\mathrm{t}} \\ \overline{g}_{\mathcal{P},l}^{C} &\geq \overline{g}_{j,l}^{vv} + v_{0,l}^{\mathrm{f}} v_{0,l}^{\mathrm{t}} - v_{0,l}^{\mathrm{f}} v_{j,l}^{\mathrm{t}} - v_{j,l}^{\mathrm{f}} v_{0,l}^{\mathrm{t}} \\ \underline{g}_{\mathcal{P},l}^{C} &\leq -\frac{1}{4} (g_{j,l}^{vv} - g_{l}^{\cos})^{2} + v_{0,l}^{\mathrm{f}} v_{0,l}^{\mathrm{t}} g_{l}^{\cos} + g_{j,l}^{vv} + v_{0,l}^{\mathrm{f}} v_{0,l}^{\mathrm{t}} \\ &- v_{0,l}^{\mathrm{f}} v_{j,l}^{\mathrm{t}} - v_{j,l}^{\mathrm{f}} v_{0,l}^{\mathrm{t}} \end{split}$$

 $\begin{array}{ll} \text{for each combination of} & g_l^{vv} \in \{\overline{g}_l^{vv},\,\underline{g}_l^{vv}\} \quad \text{and} \quad g_{i,l}^{\sin} \in \{\overline{g}_{i,l}^{\cos},\,\underline{g}_{i,l}^{\cos}\}. \end{array}$

E. Interval Bounds for $v^f v^t \sin \varphi$

The function $\psi^S = v^{\mathrm{f}}v^{\mathrm{t}}\sin\varphi$ and $g^S = v^{\mathrm{f}}v^{\mathrm{t}}\sin\varphi - v_0^{\mathrm{f}}v_0^{\mathrm{t}}\varphi$ over $v_i \in [\underline{v}_i, \overline{v}_i]$ and $\varphi_l \in [\underline{\varphi}_l, \overline{\varphi}_l]$ are bounded by the following inequalities for all $l \in \mathcal{E}$:

$$\begin{split} \overline{\psi}_{\mathcal{P},l}^{S} &\geq \frac{1}{4} (g_{l}^{vv} + g_{i,l}^{\sin})^{2} + v_{0,l}^{\mathrm{f}} v_{0,l}^{\mathrm{t}} g_{i,l}^{\sin} \\ \underline{\psi}_{\mathcal{P},l}^{S} &\leq -\frac{1}{4} (g_{l}^{vv} - g_{i,l}^{\sin})^{2} + v_{0,l}^{\mathrm{f}} v_{0,l}^{\mathrm{t}} g_{i,l}^{\sin} \\ \overline{g}_{\mathcal{P},l}^{S} &\geq \frac{1}{4} (g_{l}^{vv} + g_{i,l}^{\sin})^{2} + v_{0,l}^{\mathrm{f}} v_{0,l}^{\mathrm{t}} g_{i,l}^{\sin} - v_{0,l}^{\mathrm{f}} v_{0,l}^{\mathrm{t}} \varphi_{i,l} \\ \underline{g}_{\mathcal{P},l}^{S} &\leq -\frac{1}{4} (g_{l}^{vv} - g_{i,l}^{\sin})^{2} + v_{0,l}^{\mathrm{f}} v_{0,l}^{\mathrm{t}} g_{i,l}^{\sin} - v_{0,l}^{\mathrm{f}} v_{0,l}^{\mathrm{t}} \varphi_{i,l} \end{split}$$

 $\begin{array}{ll} \text{for each combination of} & g_l^{vv} \in \{\overline{g}_l^{vv},\,\underline{g}_l^{vv}\} \quad \text{and} \quad g_{i,l}^{\sin} \in \{\overline{g}_{i,l}^{\sin},\,\underline{g}_{i\,l}^{\sin}\}. \end{array}$

F. Interval Bounds for v^2

The function $\psi^Q = v^2$ and $g^Q = v^2 - 2v_0v$ over $v_i \in [\underline{v}_i, \overline{v}_i]$ are bounded by the following inequalities for all $k \in \mathcal{N}$:

$$\overline{\psi}_{\mathcal{P},k}^{Q} \ge v_k^2$$

$$\underline{\psi}_{\mathcal{P},k}^{Q} \le 2v_0v_k - v_0^2$$

$$\overline{g}_{\mathcal{P},k}^{Q} \ge v_k^2 - 2v_0v_k$$

$$g_{\mathcal{P},k}^{Q} \le -v_0^2$$

where $v_k \in \{\overline{v}_k, \underline{v}_k\}$.

REFERENCES

- T. Van Cutsem and C. Vournas, Voltage Stability of Electric Power Systems, vol. 441. Boston, MA, USA: Springer, 1998.
- P. Kundur, N. J. Balu, and M. G. Lauby, *Power System Stability and Control*, vol. 7. New York, NY, USA: McGraw-Hill, 1994.
- [3] B. C. Lesieutre and I. A. Hiskens, "Convexity of the set of feasible injections and revenue adequacy in FTR markets," *IEEE Trans. Power Syst.*, vol. 20, no. 4, pp. 1790–1798, Nov. 2005.
- [4] K. Lehmann, A. Grastien, and P. Van Hentenryck, "AC-feasibility on tree networks is NP-hard," *IEEE Trans. Power Syst.*, vol. 31, no. 1, pp. 798– 801, Jan. 2016.

- [5] S. H. Low, "Convex relaxation of optimal power flow—Part I: Formulations and equivalence," *IEEE Trans. Control Netw. Syst.*, vol. 1, no. 1, pp. 15–27, Mar. 2014.
- [6] J. Lavaei and S. H. Low, "Zero duality gap in optimal power flow problem," IEEE Trans. Power Syst., vol. 27, no. 1, pp. 92–107, Feb. 2012.
- [7] C. Coffrin, H. L. Hijazi, and P. Van Hentenryck, "The QC relaxation: A theoretical and computational study on optimal power flow," *IEEE Trans. Power Syst.*, vol. 31, no. 4, pp. 3008–3018, Jul. 2016.
- [8] B. Cui and X. A. Sun, "A new voltage stability-constrained optimal power-flow model: Sufficient condition, SOCP representation, and relaxation," *IEEE Trans. Power Syst.*, vol. 33, no. 5, pp. 5092–5102, Sep. 2018.
- [9] D. K. Molzahn, "Computing the feasible spaces of optimal power flow problems," *IEEE Trans. Power Syst.*, vol. 32, no. 6, pp. 4752–4763, Nov. 2017
- [10] F. Wu and S. Kumagai, "Steady-state security regions of power systems," IEEE Trans. Circuits Syst., vol. CAS-29, no. 11, pp. 703–711, Nov. 1982.
- [11] S. Bolognani and S. Zampieri, "On the existence and linear approximation of the power flow solution in power distribution networks," *IEEE Trans. Power Syst.*, vol. 31, no. 1, pp. 163–172, Jan. 2016.
- [12] S. Yu, H. D. Nguyen, and K. S. Turitsyn, "Simple certificate of solvability of power flow equations for distribution systems," in *Proc. IEEE Power Amp; Energy Soc. Gen. Meeting*. 2015, pp. 1–5.
- [13] C. Wang, A. Bernstein, J.-Y. Le Boudec, and M. Paolone, "Explicit conditions on existence and uniqueness of load-flow solutions in distribution networks," *IEEE Trans. Smart Grid*, vol. 9, no. 2, pp. 953–962, Mar. 2018.
- [14] C. Wang, A. Bernstein, J.-Y. Le Boudec, and M. Paolone, "Existence and uniqueness of load-flow solutions in three-phase distribution networks," *IEEE Trans. Power Syst.*, vol. 32, no. 4, pp. 3319–3320, Jul. 2017.
- [15] K. Dvijotham, E. Mallada, and J. W. Simpson-Porco, "High-voltage solution in radial power networks: Existence, properties, and equivalent algorithms," *IEEE Control Syst. Lett.*, vol. 1, no. 2, pp. 322–327, Oct. 2017.
- [16] J. W. Simpson-Porco, "A theory of solvability for lossless power flow equations-Part I: Fixed-point power flow," *IEEE Trans. Control Netw. Syst.*, vol. 5, no. 3, pp. 1361–1372, Sep. 2018.
- [17] J. W. Simpson-Porco, F. Dörfler, and F. Bullo, "Voltage collapse in complex power grids," *Nature Commun.*, vol. 7, 2016, Art. no. 10790.
- [18] K. Dvijotham and K. Turitsyn, "Construction of power flow feasibility sets," 2015, arXiv:1506.07191.
- [19] K. Dvijotham, H. Nguyen, and K. Turitsyn, "Solvability regions of affinely parameterized quadratic equations," *IEEE Control Syst. Lett.*, vol. 2, no. 1, pp. 25–30, Jan. 2018.
- [20] H.-D. Chiang and C.-Y. Jiang, "Feasible region of optimal power flow: Characterization and applications," *IEEE Trans. Power Syst.*, vol. 33, no. 1, pp. 236–244, Jan. 2018.
- [21] H. D. Nguyen, K. Dvijotham, and K. Turitsyn, "Constructing convex inner approximations of steady-state security regions," *IEEE Trans. Power Syst.*, vol. 34, no. 1, pp. 257–267, Jan 2019.
- [22] H. Hijazi, C. Coffrin, and P. V. Hentenryck, "Convex quadratic relaxations for mixed-integer nonlinear programs in power systems," *Math. Program. Comput.*, vol. 9, no. 3, pp. 321–367, Sep. 2017.
- [23] R. E. Moore, R. B. Kearfott, and M. J. Cloud, *Introduction to Interval Analysis*, vol. 110. Philadelphia, PA, USA: SIAM, 2009.
- [24] L. Jaulin, M. Kieffer, O. Didrit, and E. Walter, Applied Interval Analysis: With Examples in Parameter and State Estimation, Robust Control and Robotics, vol. 1. London, U.K.: Springer, 2001.
- [25] A. Goldsztejn, "A right-preconditioning process for the formal–algebraic approach to inner and outer estimation of ae-solution sets," *Rel. Comput.*, vol. 11, no. 6, pp. 443–478, 2005.
- [26] A. Goldsztejn and L. Jaulin, "Inner and outer approximations of existentially quantified equality constraints," in *Proc. Int. Conf. Principles Pract. Constraint Program.*, 2006, pp. 198–212.
- [27] M. Olivier, É. Goubault, M. Kieffer, and S. Putot, "General inner approximation of vector-valued functions," 2013, arXiv:1310.1709.
- [28] R. D. Zimmerman et al., "MATPOWER: Steady-state operations, planning, and analysis tools for power systems research and education," *IEEE Trans. Power Syst.*, vol. 26, no. 1, pp. 12–19, Feb. 2011.
- [29] J. Ortega and W. Rheinboldt, *Iterative Solution of Nonlinear Equations in Several Variables*. Philadelphia, PA, USA: SIAM, 2000.
- [30] D. Mehta, D. K. Molzahn, and K. Turitsyn, "Recent advances in computational methods for the power flow equations," in *Proc. Amer. Control Conf.*, 2016, pp. 1753–1765.
- [31] M. Tawarmalani, J.-P. P. Richard, and C. Xiong, "Explicit convex and concave envelopes through polyhedral subdivisions," *Math. Program.*, vol. 138, no. 1/2, pp. 531–577, 2013.

- [32] S. Boyd and L. Vandenberghe, Convex Optimization. Cambridge, U.K.: Cambridge Univ. Press, 2004.
- [33] I. Dunning, J. Huchette, and M. Lubin, "JuMP: A modeling language for mathematical optimization," SIAM Rev., vol. 59, no. 2, pp. 295–320, 2017.



Dongchan Lee received the B.A.Sc in engineering science and the M.A.Sc. degree in electrical and computer engineering from the University of Toronto, Toronto, ON, Canada, in 2016 and 2014, respectively. He is currently working toward the Ph.D. degree in mechanical engineering from the Massachusetts Institute of Technology (MIT), Cambridge, MA, USA.

He worked at the Independent Electricity System Operator (IESO), Toronto, in 2013, and was a Visiting Student at Los Alamos National Lab-

oratory in 2017. His current research interests are optimization, control, and power systems.



Hung D. Nguyen received the Ph.D. degree in mechanical engineering from the Massachusetts Institute of Technology (MIT), Cambridge, MA, USA, in 2017.

Currently, he is an Assistant Professor in Electrical and Electronic Engineering with Nanyang Technological University (NTU), Singapore, and the Cluster Director of Power Systems in Energy Research Institute, NTU. He is also a Visiting Professor with the Hanoi University of Science and Technology, Hanoi, Vietnam. His current re-

search interests include complex systems, nonlinear dynamics and stability, power systems and smart grids, energy storage, and personal cooling.

Dr. Nguyen was the recipient of the Siebel Scholar Class Award of 2017 on Energy Science.



Krishnamurthy Dvijotham received the bachelors degree from the Indian Institute of Technology Bombay, Mumbai, India, in 2008, and the Ph.D. degree from the University of Washington, Seattle, WA, USA, in 2014.

He is a Senior Research Scientist at Deep-Mind, London, U.K., working on robust and verifiable Al. He has held positions at Pacific Northwest National Laboratory, Richland, WA, USA; Los Alamos National Laboratory, Los Alamos, NM, USA; and the California Institute

of Technology, Pasadena, CA, USA, previously. His research research interests include machine learning, optimization and control with applications in recommendation systems, mobile devices, and power grids.

Dr. Dvijotham was the recipient of several best paper awards at top conferences in machine learning and control.



Konstantin Turitsyn received the M.Sc. degree in physics from the Moscow Institute of Physics and Technology, Dolgoprudny, Russia, in 2004, and the Ph.D. degree in physics from the Landau Institute for Theoretical Physics, Moscow, Russia, in 2007.

He was an Associate Professor with the Mechanical Engineering Department, Massachusetts Institute of Technology (MIT), Cambridge, MA, USA, until 2018. Before joining MIT, he held the position of Oppenheimer Fellow with

Los Alamos National Laboratory, Los Alamos, NM, USA, and Kadanoff Rice Postdoctoral Scholar with the University of Chicago, Chicago, IL, USA. His research interests encompass a broad range of problems involving nonlinear and stochastic dynamics of complex systems. Specific interests in energy-related fields include stability and security assessment as well as the integration of distributed and renewable generation.